

Subleading N_c improved Parton Showers

Simon Plätzer ^a and Malin Sjödal ^b

^a *DESY,
Notkestrasse 85, D-22607 Hamburg, Germany*

^b *Dept. of Astronomy and Theoretical Physics, Lund University,
Sölvegatan 14A, SE-223 62 Lund, Sweden*

ABSTRACT: We describe an algorithm for improving subsequent parton shower emissions by full SU(3) color correlations in the framework of a dipole-type shower. As a proof of concept, we present results from the first implementation of such an algorithm for a final state shower. The corrections are found to be small for event shapes and jet rates but can be more significant for tailored observables.

KEYWORDS: QCD, Jets, Parton Showers.

Contents

1. Introduction	1
2. Dipole Factorization and Dipole Shower Evolution	2
3. Color Matrix Element Corrections	5
4. Color Basis Treatment	7
5. Results	8
6. Conclusions and Outlook	14

1. Introduction

Parton showers and event generators are indispensable tools for predicting and understanding collider results [1–3]. Considering their importance for interpreting LHC results, it is essential to have a good understanding of their approximations and limitations.

Significant progress has been made over the last years in the areas of matrix element merging at leading order [4–9], and matching at next to leading order [10–15], as well as improvements to shower algorithms using dipole-type evolution [16–20], partly generalizing ideas presented originally in [21]. There has also been theoretical progress in the direction of treating full SU(3) at the level of shower evolution [22], and at the level of dealing with the color space [22–24].

In dipole-type parton showers, only large N_c color connected partons¹ can radiate coherently. The, typically $1/N_c^2$ suppressed, coherent emission from other non-color neighboring partons is neglected. However, as the number of perturbatively emitted partons n increases, the number of possible contributions from non color neighbors grows roughly like $n^2/2$, while the number of possible coherent emissions from color neighbors grows only like n . With the higher multiplicities at high energy hadron colliders, these color suppressed contributions may thus become important, though this counting does not include the dynamics of multiple parton emission. A treatment

¹‘Color connected’ here means that two partons share a common color line as used in the double line notation. Note that the double line notation can be extended beyond the large N_c limit when including an appropriate singlet contribution for the color structure of the each gluon propagator.

of these color suppressed contributions within a full-fledged shower framework is thus necessary.

This paper reports on a first step in the direction of incorporating color suppressed contributions by iterative use of color matrix element corrections. We outline an algorithm to calculate these color matrix element corrections to improve shower emissions by the full SU(3) color correlations and present a proof of concept implementation based on the shower implementation described in [15,20]. The first results are presented for $e^+e^- \rightarrow \text{jets}$.

For the implementation, a C++ color algebra package, `ColorFull` [25], has been developed for keeping track of the color structure and aiding calculation of high multiplicity matrix elements squared and color correlated matrix elements. It has also been necessary to consider the treatment of negative weights in the context of parton showers, as there are negative contributions to the radiation probability from color suppressed terms [26].

This paper is organized as follows: in Sec. 2 we recapitulate the dipole factorization scheme and the dipole shower evolution. In Sec. 3 we define an algorithm for the inclusion of full color correlations for subsequent parton shower emissions. The details of the color space treatment are given in Sec. 4. In Sec. 5 we present numerical results from the implementation of a parton shower improved by full color correlations. Sec. 6 draws some conclusions and gives an outlook on future developments.

2. Dipole Factorization and Dipole Shower Evolution

Dipole factorization, [27,28], states that the behavior of QCD tree-level matrix elements squared in any singly unresolved limit involving two partons i, j (*i.e.* whenever i and j become collinear or one of them soft), can be cast into the form

$$|\mathcal{M}_{n+1}(\dots, p_i, \dots, p_j, \dots, p_k, \dots)|^2 \approx \sum_{k \neq i, j} \frac{1}{2p_i \cdot p_j} \langle \mathcal{M}_n(\dots, p_{\tilde{i}j}, \dots, p_{\tilde{k}}, \dots) | \mathbf{V}_{ij,k}(p_i, p_j, p_k) | \mathcal{M}_n(\dots, p_{\tilde{i}j}, \dots, p_{\tilde{k}}, \dots) \rangle, \quad (2.1)$$

where $|\mathcal{M}_n\rangle$ – which is a vector in the space of helicity and color configurations – denotes the amplitude for an n -parton final state. Here an emitter $\tilde{i}j$ undergoes splitting to two partons i and j in the presence of a spectator \tilde{k} which absorbs the longitudinal recoil of the splitting, $\tilde{k} \rightarrow k$, such as to keep the momenta both before and after emission on their mass shell while maintaining exact energy-momentum conservation. Considering gluon emission only, this can be interpreted as a dipole $\tilde{i}j, \tilde{k}$ emitting a gluon of momentum p_j . (However, $g \rightarrow \bar{q}q$ splittings fit into this framework without conceptual changes).

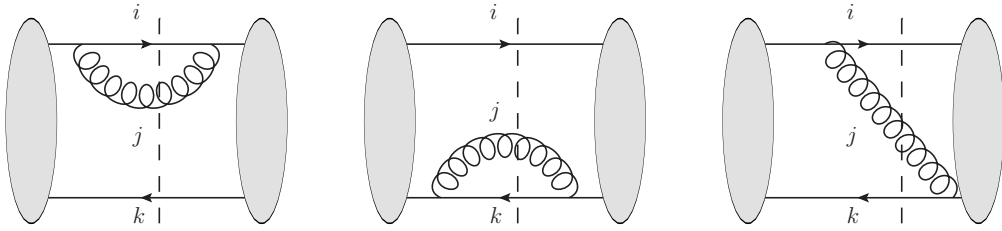


Figure 1: Sample diagrams contributing to the dipole kernels $\mathbf{V}_{ij,k}$ and $\mathbf{V}_{kj,i}$ in the singular limits for gluon emission off a quark or antiquark. Similar diagrams are present for gluon splittings.

In general, the insertion operator \mathbf{V} contains both color correlations stemming from soft gluon emissions and spin correlations originating in the collinear splitting of a gluon. We shall limit ourselves to massless quarks and color correlations only, using the spin averaged dipole splitting functions presented in [28]. In this case

$$\mathbf{V}_{ij,k}(p_i, p_j, p_k) = -8\pi\alpha_s V_{ij,k}(p_i, p_j, p_k) \frac{\mathbf{T}_{\tilde{i}\tilde{j}} \cdot \mathbf{T}_k}{\mathbf{T}_{\tilde{i}\tilde{j}}^2} \quad (2.2)$$

in terms of the color charge operators \mathbf{T}_i^2 . This notation is independent of the basis considered for color space, though we shall stick to one particular choice of basis, to be discussed in Sec. 4.

The kernel $V_{ij,k}$ only contains a collinear enhancement with respect to the splitting $\tilde{i}\tilde{j} \rightarrow i, j$. It is constructed by rearranging singular contributions of sets of diagrams as depicted in Fig. 1 while making use of the fact that the amplitude is a color singlet,

$$\mathbf{T}_{\tilde{i}\tilde{j}}^2 = - \sum_{k \neq \tilde{i}\tilde{j}} \mathbf{T}_{\tilde{i}\tilde{j}} \cdot \mathbf{T}_k. \quad (2.3)$$

For gluon emission off a final-final dipole configuration, the case considered in the present paper, the kernels read

$$V_{qg,k}(p_i, p_j, p_k) = C_F \left(\frac{2(1-z)}{(1-z)^2 + p_{\perp}^2/s_{ijk}} - (1+z) \right) \quad (2.4)$$

$$V_{gg,k}(p_i, p_j, p_k) = 2C_A \left(\frac{1-z}{(1-z)^2 + p_{\perp}^2/s_{ijk}} + \frac{z}{z^2 + p_{\perp}^2/s_{ijk}} - 2 + z(1-z) \right) \quad (2.5)$$

where we have introduced the relative scalar transverse momentum p_{\perp} and longitudinal momentum fraction z of parton i as given by the Sudakov decomposition

²We use the conventions on the color charge algebra as given in [28]. Note that the Casimir operators $\mathbf{T}_i^2 = C_F$ if i is an (anti-)quark, and $\mathbf{T}_i^2 = C_A$ if i is a gluon are included in the definition of the splitting kernels V ; thus the color correlations are normalized accordingly. This convention is more transparent when comparing to parton showers in the large N_c limit to be discussed below.

$$p_i = zp_{\tilde{i}j} + \frac{p_{\perp}^2}{zs_{ijk}}p_{\tilde{k}} + k_{\perp} \quad (2.6)$$

$$p_j = (1-z)p_{\tilde{i}j} + \frac{p_{\perp}^2}{(1-z)s_{ijk}}p_{\tilde{k}} - k_{\perp} \quad (2.7)$$

$$p_k = \left(1 - \frac{p_{\perp}^2}{z(1-z)s_{ijk}}\right)p_{\tilde{k}}, \quad (2.8)$$

with $p_{\tilde{i}j}^2 = p_{\tilde{k}}^2 = 0$, a space like transverse momentum k_{\perp} with $k_{\perp}^2 = -p_{\perp}^2$ and $k_{\perp} \cdot p_{\tilde{i}j} = k_{\perp} \cdot p_{\tilde{k}} = 0$. With this parametrization we also have $s_{ijk} = (p_i + p_j + p_k)^2 = (p_{\tilde{i}j} + p_{\tilde{k}})^2$.

Reinterpreting the dipole factorization in terms of emitting dipoles, parton cascades can be based on it and, after slight modifications to initial state radiation, have been shown to exhibit the proper features in terms of coherent gluon emission and logarithmic accuracy [20]. The present work is an extension to the implementation of a coherent dipole evolution, details of which have been reported in [15]. Besides using spin averaged dipole kernels – like any other parton shower implementation available so far – the Monte Carlo implementation in [15] treats the color correlation operator for the shower in the large N_c limit *i.e.* when using the double line notation of color

$$-\frac{\mathbf{T}_{\tilde{i}j} \cdot \mathbf{T}_k}{\mathbf{T}_{\tilde{i}j}^2} \rightarrow \frac{1}{1 + \delta_{\tilde{i}j}} \delta(\tilde{i}j, k \text{ color connected}), \quad (2.9)$$

where $\delta_{\tilde{i}j} = 1$ if $\tilde{i}j$ is a gluon, and vanishes otherwise. Here the initial assignment and further evolution of large N_c color charge flow is extensively discussed in *e.g.* [15]. Let us only recall here that to each of the two emitter-spectator partitions of a large N_c color connected pair of partons we connect an emission probability related to the dipole kernels $V_{ij,k}$ as

$$dP_{ij,k}(p_{\perp}^2, z; p_{\tilde{i}j}, p_{\tilde{k}}) = \frac{\alpha_s}{2\pi} \frac{dp_{\perp}^2}{p_{\perp}^2} dz \mathcal{J}(p_{\perp}^2, z; p_{\tilde{i}j}, p_{\tilde{k}}) V_{ij,k}(p_{\perp}^2, z; p_{\tilde{i}j}, p_{\tilde{k}}). \quad (2.10)$$

Here, \mathcal{J} represents the Jacobian for changing variables from p_i, p_j, p_k to $p_{\tilde{i}j}, p_{\tilde{k}}, p_{\perp}, z$ and an azimuthal orientation, which has been integrated over. For a final-final dipole configuration, $\mathcal{J}(p_{\perp}^2, z; p_{\tilde{i}j}, p_{\tilde{k}}) = (1 - p_{\perp}^2/z(1-z)s_{ijk})$.

In this paper we report on generalizing this picture from large N_c color connected dipoles to all pairs of partons, taking into account the exact evaluation of the color correlations. Thus, the notion of dipole chains and their splittings does not apply anymore. Instead every pair of partons has to be considered competing for the next emission. Details of the generalized algorithm are given in Sec. 3 below.

3. Color Matrix Element Corrections

Following the arguments of how a parton cascade is constructed from the dipole factorization formula (2.1), we may recast (2.10) to include the exact color correlations by assigning splitting rates

$$dP_{ij,k}(p_{\perp}^2, z; p_{\tilde{i}j}, p_{\tilde{k}}) = \frac{\alpha_s}{2\pi} \frac{dp_{\perp}^2}{p_{\perp}^2} dz \mathcal{J}(p_{\perp}^2, z; p_{\tilde{i}j}, p_{\tilde{k}}) V_{ij,k}(p_{\perp}^2, z; p_{\tilde{i}j}, p_{\tilde{k}}) \times \frac{-1}{\mathbf{T}_{\tilde{i}j}^2} \frac{\langle \mathcal{M}_n | \mathbf{T}_{\tilde{i}j} \cdot \mathbf{T}_k | \mathcal{M}_n \rangle}{|\mathcal{M}_n|^2} \quad (3.1)$$

to *each pair* $\tilde{i}j, \tilde{k}$ of partons to generate an emission j off an n -parton system. In the large N_c limit the factor after the times sign reduces to (2.9) for color connected pairs of partons and zero otherwise. Here, by allowing any pair of partons to radiate, it accounts for correcting the emission to include the exact color correlations. Owing to the similarity to so-called matrix element corrections present in parton showers, [29, 30], we refer to this improvement as *color matrix element corrections*.

At the level of the hard process, from which the shower evolution is starting, the calculation of $|\mathcal{M}_n\rangle$ is straightforward, but once the first emission is performed, the issue of how to describe the evolved state has to be addressed. By picking a particular basis for the color structures, we can map $|\mathcal{M}_n\rangle$ to a complex vector $\mathcal{M}_n \in \mathbb{C}^{d_n}$, where d_n is the dimensionality of the basis for n partons,

$$|\mathcal{M}_n\rangle = \sum_{\alpha=1}^{d_n} c_{n,\alpha} |\alpha_n\rangle \quad \leftrightarrow \quad \mathcal{M}_n = (c_{n,1}, \dots, c_{n,d_n})^T \quad (3.2)$$

Then we have

$$|\mathcal{M}_n|^2 = \mathcal{M}_n^\dagger S_n \mathcal{M}_n = \text{Tr} (S_n \times \mathcal{M}_n \mathcal{M}_n^\dagger) \quad (3.3)$$

with S_n being the scalar product matrix, $(S_n)_{\alpha\beta} = \langle \alpha_n | \beta_n \rangle$, for color basis vectors $|\alpha_n\rangle$ and $|\beta_n\rangle$. Moreover, the color correlated matrix element for emission from $\tilde{i}j$ and \tilde{k} can be written as

$$\langle \mathcal{M}_n | \mathbf{T}_{\tilde{i}j} \cdot \mathbf{T}_{\tilde{k}} | \mathcal{M}_n \rangle = \text{Tr} (S_{n+1} \times T_{\tilde{k},n} \mathcal{M}_n \mathcal{M}_n^\dagger T_{\tilde{i}j,n}^\dagger) \quad (3.4)$$

in terms of matrix representations of $\mathbf{T}_{\tilde{i}j}, \mathbf{T}_{\tilde{k}} \in \mathbb{C}^{d_{n+1}, d_n}$. These matrices describe the color space effect of emission from the partons $\tilde{i}j$ and \tilde{k} by mapping a basis tensor in n -parton space to a linear combination of basis tensors in $n+1$ -parton space. In the "trace basis", which is used here, (c.f. Sec. 4) the $\mathbf{T}_{\tilde{i}j}$ matrices are very sparse [22, 23]. The scalar product matrices, S_n, S_{n+1} , are however dense, and the calculations of these matrices is a key ingredient for running a parton shower improved by color matrix element corrections.

As we want to keep the full color structure the evolution is (analogous to [22]) done keeping the amplitude information, using a matrix M_n , which initially – for

the hard process the shower starts with – is given by $M_n = \mathcal{M}_n \mathcal{M}_n^\dagger$. After having performed an emission with momentum p_j off an n -parton configuration, this quantity for the $n + 1$ parton configuration can then be obtained from the spin-averaged dipole kernel as

$$M_{n+1} = - \sum_{i \neq j} \sum_{k \neq i, j} \frac{4\pi\alpha_s V_{ij,k}(p_i, p_j, p_k)}{p_i \cdot p_j \mathbf{T}_{ij}^2} T_{\tilde{k},n} M_n T_{\tilde{i}j,n}^\dagger. \quad (3.5)$$

Matrix elements squared and color correlated matrix elements for each subsequent color matrix element correction are then calculated as in (3.3) and (3.4) upon replacing $\mathcal{M}_n \mathcal{M}_n^\dagger \rightarrow M_n$. One property of the color matrix element correction weight is that it is not necessarily positive definite for subleading- N_c contributions. The authors have shown in [26], that this does not pose a problem for a Monte Carlo implementation. In particular, from the very definition of the dipole factorization as an approximation to a tree-level matrix element squared, the sum of the splitting probabilities including all pairs i, k is strictly positive definite. Thus we can immediately apply the interleaved competition/veto algorithm [26] to generate kinematic variables with the desired density.

More precisely we select a set of candidate emissions $\tilde{i}j, \tilde{k} \rightarrow i, j, k$ at scales $p_{\perp, \tilde{i}j, k}$ (when starting from a scale Q_\perp^2 associated with the dipole $\tilde{i}j, \tilde{k}$) according to the Sudakov form factor

$$-\ln \Delta_{ij,k}(p_{\perp, ij, k}^2 | Q_\perp^2) = \frac{\alpha_s}{2\pi} \int_{p_{\perp, ij, k}^2}^{Q_\perp^2} \frac{dq_\perp^2}{q_\perp^2} \int_{z_-(q_\perp^2, Q_\perp^2)}^{z_+(q_\perp^2, Q_\perp^2)} dz \mathcal{P}_{ij,k}(q_\perp^2, z; p_{\tilde{i}j}, p_{\tilde{k}}), \quad (3.6)$$

if $\mathcal{P}_{ij,k}$ is positive. Here, in accordance with (3.1),

$$\mathcal{P}_{ij,k}(p_\perp^2, z; p_{\tilde{i}j}, p_{\tilde{k}}) = \mathcal{J}(p_\perp^2, z; p_{\tilde{i}j}, p_{\tilde{k}}) V_{ij,k}(p_\perp^2, z; p_{\tilde{i}j}, p_{\tilde{k}}) \times \frac{-1}{\mathbf{T}_{\tilde{i}j}^2} \frac{\langle \mathcal{M}_n | \mathbf{T}_{\tilde{i}j} \cdot \mathbf{T}_k | \mathcal{M}_n \rangle}{|\mathcal{M}_n|^2} \quad (3.7)$$

and $z_\pm(p_\perp^2, Q_\perp^2) = (1 \pm \sqrt{1 - p_\perp^2/Q_\perp^2})/2$. Amongst the candidate splittings of $\tilde{i}j, \tilde{k}$, we pick the one with largest $p_{\perp, \tilde{i}j, k}^2 = p_\perp^2$ and accept the corresponding splitting with probability

$$\frac{\sum_{\tilde{i}j} \sum_{\tilde{k} \neq \tilde{i}j} \mathcal{P}_{ij,k}(p_\perp^2, z; p_{\tilde{i}j}, p_{\tilde{k}})}{\sum_{\tilde{i}j} \sum_{\tilde{k} \neq \tilde{i}j} \mathcal{P}_{ij,k}(p_\perp^2, z; p_{\tilde{i}j}, p_{\tilde{k}}) \theta(\mathcal{P}_{ij,k}(p_\perp^2, z; p_{\tilde{i}j}, p_{\tilde{k}}))}. \quad (3.8)$$

Upon rejection, the selection is repeated, setting $Q_\perp = p_\perp$, until the next p_\perp is accepted or eventually p_\perp is found at the infrared cutoff $\mu = \mathcal{O}(1 \text{ GeV})$. Upon accepting the candidate splitting with scale p_\perp , the dipole $\tilde{i}j, \tilde{k}$ is chosen to define the Sudakov decomposition of the emission kinematics. The generated emission is then inserted into the event record, and M_{n+1} is determined using the generated kinematics according to (3.5).

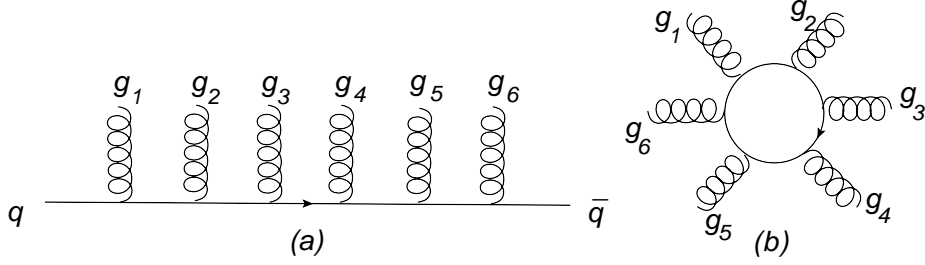


Figure 2: Examples of color structures. (a): An open quark line with 6 gluons corresponding to the color structure $t_{qq_1}^{g_1} t_{q_1 q_2}^{g_2} t_{q_2 q_3}^{g_3} t_{q_3 q_4}^{g_4} t_{q_4 q_5}^{g_5} t_{q_5 \bar{q}}^{g_6}$. This is the only type of color structure needed for $e^+e^- \rightarrow q\bar{q} \rightarrow q\bar{q} + N_g$ gluons at leading order. (b) A closed quark line corresponding to the color structure $t_{q_6 q_1}^{g_1} t_{q_1 q_2}^{g_2} t_{q_2 q_3}^{g_3} t_{q_3 q_4}^{g_4} t_{q_4 q_5}^{g_5} t_{q_5 q_6}^{g_6} = \text{Tr} [t^{g_1} t^{g_2} t^{g_3} t^{g_4} t^{g_5} t^{g_6}]$.

4. Color Basis Treatment

Throughout this paper we use the basis obtained by first connecting all $q\bar{q}$ -pairs in all possible ways (for one $q\bar{q}$ -pair only one way), and then attaching gluons to the quark-lines in all possible ways ($N_g!$ ways for one $q\bar{q}$ -pair), see Fig. 2a. This basis is sufficient as long as only leading order QCD processes are considered. In the presence of (QCD) virtual corrections, or processes mediated by electroweak (or other color singlet) exchanges, we would also have to consider basis vectors obtained from direct products of open and closed quark-lines, as depicted in Fig. 2.

Due to the relation

$$if_{abc} = \frac{1}{T_R} (\text{Tr}[t^a t^b t^c] - \text{Tr}[t^b t^a t^c]) = \frac{1}{T_R} (t_{q_1 q_2}^a t_{q_2 q_3}^b t_{q_3 q_1}^c - t_{q_1 q_2}^b t_{q_2 q_3}^a t_{q_3 q_1}^c) \quad (4.1)$$

where $T_R = \text{Tr}[t^a t^a]$ (no sum) is taken to be $1/2$, the effect of gluon emission and gluon exchange is trivial in this basis [22, 23]. Graphically the emission process can be exemplified as in Fig. 3. Using the notation

$$|\{q g_1 g_2 \dots g_m \bar{q}\}\rangle = t_{q, q_1}^{g_1} t_{q_1, q_2}^{g_2} \dots t_{q_{m-1}, \bar{q}}^{g_m} \quad (4.2)$$

we may in general write for the emission of gluon g_{n+1} from the gluon at place i

$$|\{q g_1 \dots \tilde{g}_i \dots g_m \bar{q}\}\rangle \rightarrow |\{q g_1 \dots g_i g_{m+1} \dots g_m \bar{q}\}\rangle - |\{q g_1 \dots g_{m+1} g_i \dots g_m \bar{q}\}\rangle \quad (4.3)$$

where the overall sign depends on the sign convention for the triple gluon vertex, and thus has to be matched with the convention for the momentum dependent part. Here we choose the triple gluon vertex factor to be $if_{\tilde{g}, g, g_{m+1}}$ where \tilde{g} denotes the emitters color index before emission, g denotes the emitters color after emission, and g_{m+1} denotes the color index of the emitted gluon. For quarks and anti-quarks the effects of gluon emission are similarly

$$|\{q g_1 \dots g_m \bar{q}\}\rangle \rightarrow |\{q g_{m+1} g_1 \dots g_m \bar{q}\}\rangle \text{ for } q \quad (4.4)$$

$$|\{q g_1 \dots g_m \bar{q}\}\rangle \rightarrow -|\{q g_1 \dots g_m g_{m+1} \bar{q}\}\rangle \text{ for } \bar{q}. \quad (4.5)$$

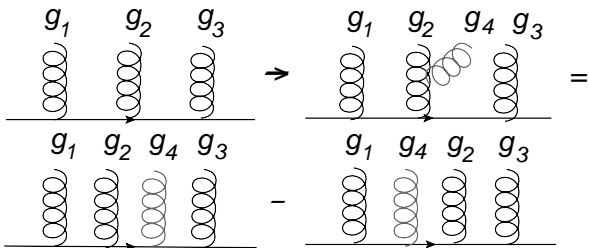


Figure 3: The graphical representation of (4.3) for $i = 2$.

The disadvantages of this type of basis – obtained by connecting partons in all possible ways – is that it is orthogonal only in the $N_c \rightarrow \infty$ limit, and that it is overcomplete for finite N_c . For $N_c = 3$ the lowest number of partons for which this kind of basis is overcomplete is four gluons (incoming plus outgoing).

We note that there are two computational steps which naively scale as $(N_g!)^2$. The first step is the step of calculating all the scalar products between the $N_g!$ basis vectors. The second is the step of identifying the new basis vectors when a given parton in a given basis vector has emitted a new gluon; the number of basis vectors in the initial basis scales as $(N_g - 1)!$ (starting from $N_g - 1$ gluons), and the number of basis vectors in the final basis as $N_g!$. This would give an overall scaling behavior of $(N_g - 1)!(N_g + 1)N_g! \sim (N_g!)^2$, as there are $(N_g + 1)$ possible emitters.

However, enumerating the basis states in a unique way, it is possible to *calculate* the numbers of the new basis vectors when a gluon has been emitted from a given parton in a given basis vector. As there is no need to compare the result after emission to all basis vectors in the N_g -basis, this reduces the computational effort to scale rather as $(N_g - 1)!(N_g + 1)$ in the step of identifying all new color states when starting in $(N_g - 1)!$ possible basis vectors and emitting from $N_g + 1$ possible emitters. This is clearly much better than the $(N_g!)^2$ scaling for calculating the scalar products, which thus is the major bottleneck for sufficiently many partons. Fortunately these calculations need only be performed once, and can then be stored numerically for use in the color matrix element corrections.

The scalar product matrices have been checked to agree with scalar product matrices calculated by the Mathematica code published along with [24] for up to 4 gluons, and against a new (yet unpublished) Mathematica package. Similarly the matrices representing $\mathbf{T}_{\tilde{i}j} \cdot \mathbf{T}_{\tilde{k}}$ have been checked to agree for up to 3 gluons compared to the old Mathematica code, and for up to 4 gluons compared to the new.

5. Results

We here discuss first results from a subleading N_c improved final state shower, originating from $e^+e^- \rightarrow q\bar{q}$ at 91 GeV center of mass energy. We consider gluon emission only, as there is no soft enhancement present for a $g \rightarrow q\bar{q}$ splitting. The strong coupling constant is taken to be fixed, $\alpha_s = 0.112$. The subsequent gluon emissions are performed as described in Sec. 3 using one of three options for the color structure:

1. **Full** color structure; the full SU(3) color structure with splitting kernels as in (3.1) is used with emissions generated as in Sec. 3.
2. **Shower** color; the color matrix element correction is evaluated in the large N_c limit, though the color factor C_F entering $q \rightarrow qg$ splittings is kept at its exact value $C_F = 4/3$. This resembles current parton shower implementations.
3. **Strict large** N_c , all N_c suppressed terms are dropped, implying $C_F = 3/2$.

Before turning to the numerical results it is instructive to study the expected effects already at an analytical level, and to clarify how the shower limit maps to the standard shower implementation. We therefore consider the correction weights for up to three emissions, labelling each intermediate state with $N_g = n - 2$ additional gluons as $q_1 \bar{q}_2 g_3 \dots g_n$. The gluon g_n , is always considered to be the one emitted in the last transition, and the weight associated to a dipole i, k in an ensemble with n partons is denoted by

$$\frac{1}{\mathbf{T}_i^2} \frac{4\pi\alpha_s}{p_i \cdot p_n} V_{in,k}(p_i, p_n, p_k) \equiv V_{ik}^n. \quad (5.1)$$

The color matrix element correction for emission off a dipole i, k in an n -parton ensemble is denoted

$$-\frac{1}{\mathbf{T}_i^2} \frac{\langle \mathcal{M}_n | \mathbf{T}_i \cdot \mathbf{T}_k | \mathcal{M}_n \rangle}{|\mathcal{M}_n|^2} = -\frac{1}{\mathbf{T}_i^2} \frac{\text{Tr} \left(S_{n+1} \times T_{i,n} M_n T_{k,n}^\dagger \right)}{\text{Tr} (S_n \times M_n)} \equiv w_{ik}^n \quad (5.2)$$

for brevity. Keeping the full correlations we find the corrections for the first two emissions to be given by

$$\begin{aligned} w_{12}^2 &= w_{21}^2 = 1 \\ w_{13}^3 &= w_{23}^3 = \frac{9}{8} \\ w_{31}^3 &= w_{32}^3 = \frac{1}{2} \\ w_{12}^3 &= w_{21}^3 = -\frac{1}{8}. \end{aligned} \quad (5.3)$$

The negative contribution from the $q\bar{q}$ dipole in the $q\bar{q}g$ system has already been noted in [31]. Note that, *e.g.* $w_{12}^3 + w_{13}^3 = 1$ as dictated by color conservation. In the shower approximation we have

$$\begin{aligned} w_{12}^2 &= w_{21}^2 = 1 \\ w_{13}^3 &= w_{23}^3 = 1 \\ w_{31}^3 &= w_{32}^3 = \frac{1}{2} \\ w_{12}^3 &= w_{21}^3 = 0 \end{aligned} \quad (5.4)$$

matching precisely the naive expectations on the subleading N_c contributions, that there is no radiation off the $q\bar{q}$ dipole in a $q\bar{q}g$ system. For the first emission there is no difference between the two approximations reflecting the triviality of the color basis in that case. Also, gluon splittings in a $q\bar{q}g$ system do not exhibit any subleading N_c correction.

More non-trivial dynamics are present for the fourth emission. Introducing the relative magnitudes of dipole kernels encountered in the four parton system with respect to the $q(\bar{q})g$ dipoles,

$$r_{ik} = \frac{V_{ik}^3 + V_{ki}^3}{V_{13}^3 + V_{31}^3 + V_{23}^3 + V_{32}^3} \quad (5.5)$$

we find for the exact correlations

$$\begin{aligned} w_{13}^4 = w_{24}^4 &= \frac{9}{8} \frac{r_{23} - \frac{1}{9}r_{12}}{1 - \frac{1}{9}r_{12}} \\ w_{14}^4 = w_{23}^4 &= \frac{9}{8} \frac{r_{13} - \frac{1}{9}r_{12}}{1 - \frac{1}{9}r_{12}} \\ w_{31}^4 = w_{42}^4 &= \frac{1}{2} \frac{r_{23} - \frac{1}{9}r_{12}}{1 - \frac{1}{9}r_{12}} \\ w_{41}^4 = w_{32}^4 &= \frac{1}{2} \frac{r_{13} - \frac{1}{9}r_{12}}{1 - \frac{1}{9}r_{12}} \\ w_{34}^4 = w_{43}^4 &= \frac{1}{2} \frac{1}{1 - \frac{1}{9}r_{12}} \\ w_{12}^4 = w_{21}^4 &= -\frac{1}{8} \frac{1 - \frac{10}{9}r_{12}}{1 - \frac{1}{9}r_{12}} . \end{aligned} \quad (5.6)$$

We note that the correction weights only depend on the quantities r_{ij} . Conversely, in the large N_c limit we find

$$\begin{aligned} w_{13}^4 = w_{24}^4 &= r_{23} \\ w_{14}^4 = w_{23}^4 &= r_{13} \\ w_{31}^4 = w_{42}^4 &= \frac{1}{2} r_{23} \\ w_{41}^4 = w_{32}^4 &= \frac{1}{2} r_{13} \\ w_{34}^4 = w_{43}^4 &= \frac{1}{2} \\ w_{12}^4 = w_{21}^4 &= 0 . \end{aligned} \quad (5.7)$$

Again, there is no radiation off the $q\bar{q}$ dipole, the gg dipole precisely matches the standard shower implementation. The different combinations of $q(\bar{q})g$ dipoles resemble the standard shower implementation only in the case that – in the three parton

system – the splitting functions of one dipole had been much larger than the splitting functions of the other dipole. In this case the weights precisely match up the distribution of radiation generated by the shower once it has decided which dipole was to radiate – this history is of course closely linked to the hierarchy of splitting kernel values encountered. Indeed, the deviations between the shower approximation and the standard shower implementation have been found to be negligible.

The shower is terminated when either the N_g :th gluon (we here consider up to $N_g = 4, 5, 6$ gluon emissions) is emitted, or when the infrared cut-off, taken to be 1 GeV, is reached. Only about 1% of all events radiate up to 6 gluons.

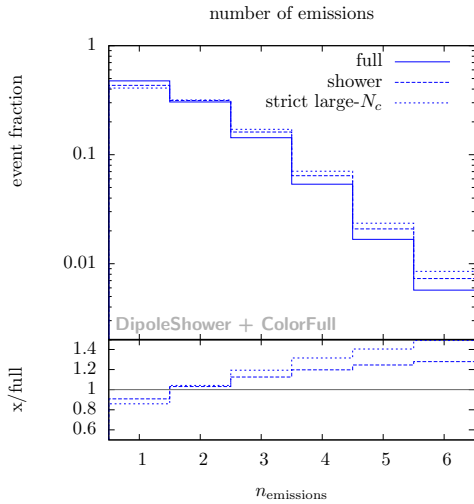


Figure 4: The normalized distribution of the number of emissions above the infrared cutoff comparing the different levels of approximation.

increased radiation probability accounts entirely for the difference between the ”strict large N_c ” and the ”shower” treatments. Apart from this effect, there is another effect which makes both the strict large N_c and the shower treatments of color, result in more radiation, compared to keeping the full color structure. This may be attributed to the fact that the interference between color structures, where two gluons cross each other, as depicted in in Fig. 5(b), comes with negative sign. These terms – which are not present in standard parton showers – thus seem to lower the probability for radiation. For a large number of emissions, color structures where gluons cross each other in more complicated ways dominate the color suppressed contributions. Starting from two $q\bar{q}$ -pairs there are terms which are only suppressed by one power of N_c . We thus caution that the effects of color suppressed terms may be significantly larger at the LHC.

For the LEP-like setting considered here, we have investigated a set of standard observables, event shapes and jet rates. In all cases we find the deviations of the shower approximation to be small, up to a few percent, when compared to the

As, due to computational limitations, we only consider a limited number of emissions, we have, for the observables considered here, checked that the prediction stabilizes when going up to six emissions. The distribution of the number of emissions is shown in Fig. 4 for the various approximations considered. We find that taking the strict large N_c limit rises the probability for many gluon emissions by more than 40%. This can in part be attributed to the fact that $C_F = T_R(N_c^2 - 1)/N_c$, which equals $4/3$ (using $T_R = 1/2$) is replaced by its leading part $3/2$ also for collinear emissions. The buildup of this increased radiation probability accounts entirely for the difference between the ”strict large N_c ” and the ”shower” treatments.

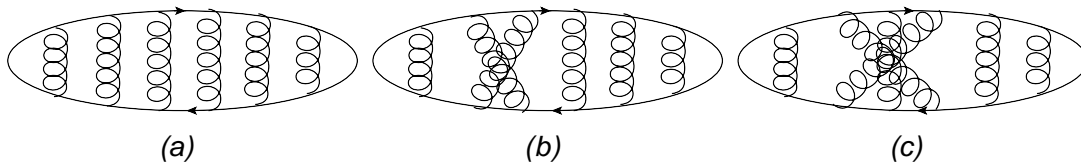


Figure 5: With diagrammatic techniques an amplitude square, as in (a) can easily be evaluated to $N_c C_F^{N_g}$. The type of interference depicted in (b), where 2 gluons cross at one point contributes negatively to the radiation probability with $-T_R C_F^{N_g-1}$, whereas the interference depicted in (c) contributes positively with $T_R^2 C_F^{N_g-2} (N_c^2 + 1)/N$.

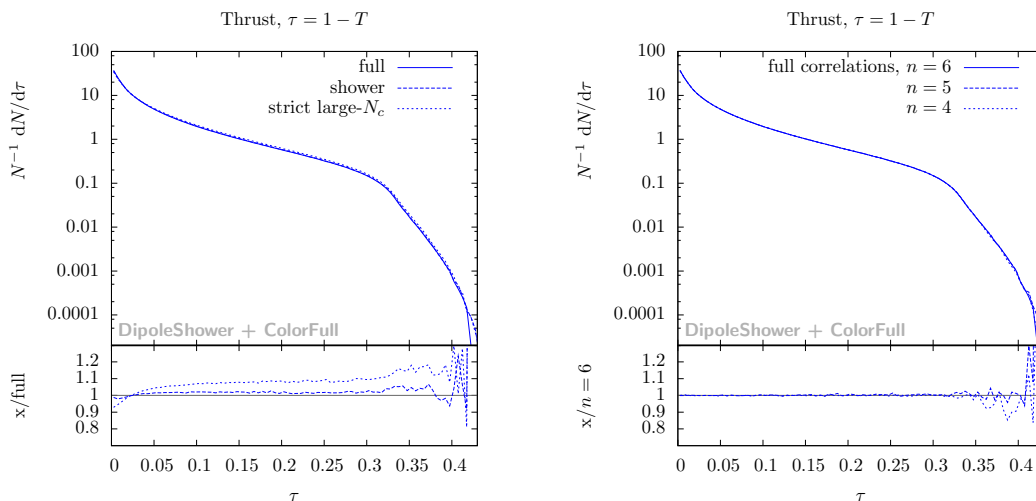


Figure 6: The distribution of one minus thrust, $\tau = 1 - T$. The left panel compares different approximations of the color structure. The right panel compares predictions depending on the number of emissions using the full color structure. The prediction stabilizes from five emissions onward, as is the case for the other observables considered.

full color treatment. The differences between the strict large N_c and the "shower" treatment option are often larger, in the cases of thrust, T , and sphericity up to roughly 10%. In Fig. 6 we show the $\tau = 1 - T$ distributions for the three options of color structure (left), and – using the full color structure – depending on how many emissions we allow (right). The right plot shows that the prediction stabilizes from five emissions onward. We note that there is not much difference between the full and the shower-like treatment of the color structure, whereas the strict large N_c treatment results in less pencil like events. This can be understood by noting that there are more emissions in this case, as indicated in Fig. 4.

We now turn our attention to differential Durham n -jet rates, Fig. 7, showing the distribution of the resolutions scale, $y = 2 \min(E_i^2, E_j^2)(1 - \cos \theta_{ij})/s$, at which an $n + 1$ -jet event changes to an n -jet event. We note that for the two-jet rate, there is almost no difference between the full and "shower" option whereas, increasing

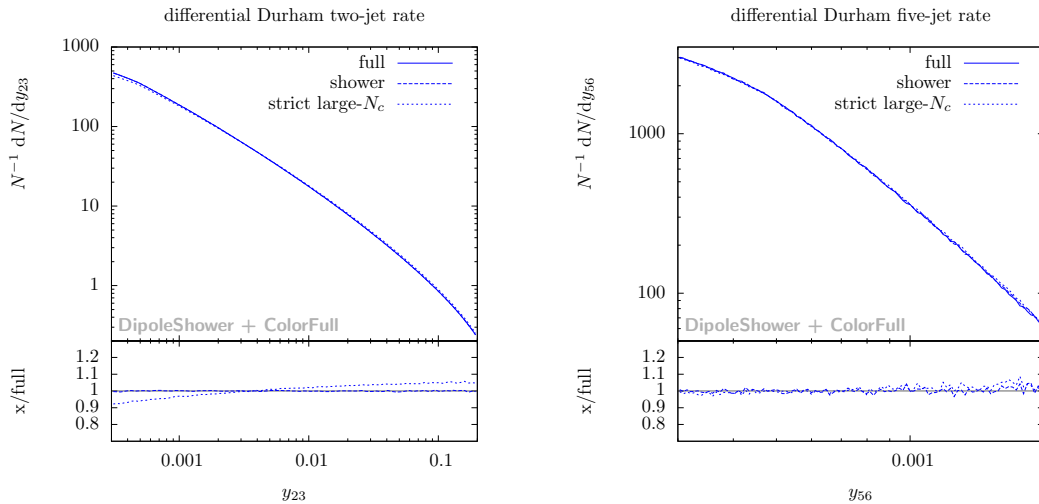


Figure 7: Durham differential n -jet rates for transition from three to two (left), and six to five jets (right).

the number of jets, we may see a few percent difference, although this difference may be just a statistical fluctuation. For the two jet rate the small difference can be understood by considering that the transition from a three to a two-jet event is *only* sensitive to the emission of a gluon from a quark-line, i.e. to C_F , which is correctly described in standard showers, as well as for the case that no non-trivial color correlations are present for the first emission. Nevertheless, the difference between shower and full remains very small, at most a few percent, for the differential n -jet observables.

In general we find that the differences between the shower approximation and full correlations are small for event shapes and jet rates considered here. The explanation for this is likely that these observables either are mainly sensitive to the collinear singularity – which is treated with the correct color factor in standard parton showers – or are mainly sensitive to the first hard emission, in case of which there are no non-trivial correlations present.

The next candidates to check for larger effects are four-jet correlations, which have been studied at LEP, mainly to investigate the non-abelian nature of QCD, *i.e.* these are all very sensitive to $g \rightarrow gg$ splittings. An example, the distribution of the cosine of the angle between the softest two jets in four-jet events at a Durham-jet resolution of $y = 0.008$ are shown in Fig. 8. No large deviations are observed between the different approximations. A closer consideration of the color space for a $q\bar{q}$ pair and two gluons reveals that this may actually be expected. Note that there is almost no difference between the shower and strict large N_c approximations, which can be attributed to the fact that these observables mainly probe gluon splitting which is not sensitive to the difference between these approximations.

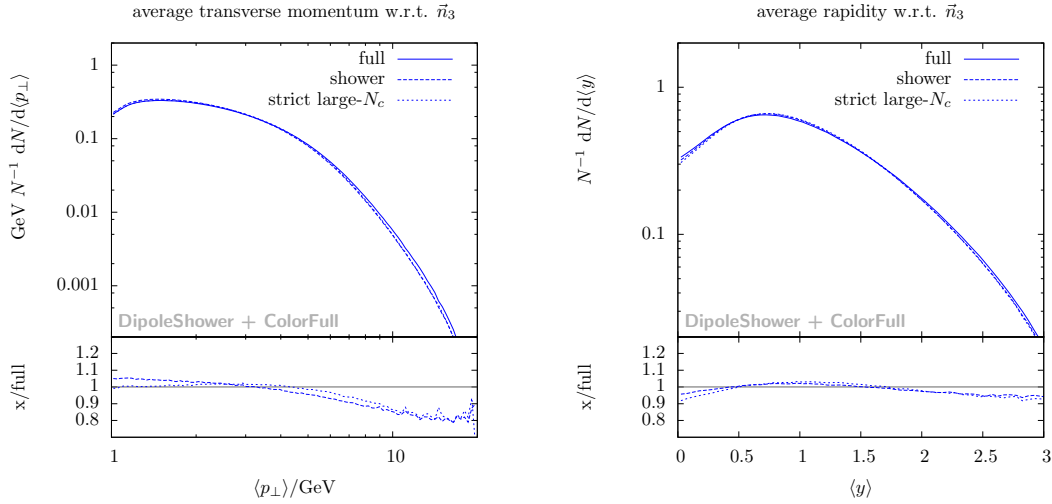


Figure 9: The average transverse momentum and rapidity of partons four onward w.r.t. the thrust axis defined by the three hardest partons.

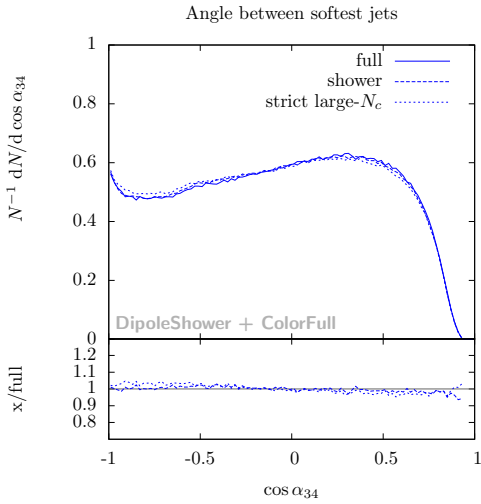


Figure 8: Distribution of the cosine of the angle between the softest jets in four-jet events.

of anti- k_{\perp} -type jets to build up a reference system from hard, collinear jets while being able to look at the orientation of soft radiation relative to this system.

6. Conclusions and Outlook

In this paper the first results from a subleading N_c parton shower were presented. We have considered final state gluon emissions using iterative matrix element corrections

To investigate the effects of soft coherent emissions, we have therefore also studied the average transverse momentum and rapidity of parton four onward with respect to the thrust axis defined by the three hardest partons. The result is shown in Fig. 9. Here the effects are much larger. We find that the average transverse momentum is harder if the full color structure is kept, for large $\langle p_{\perp} \rangle$ up to 20%. We also see that the strict large N_c approximation is somewhat closer to the prediction including the full correlations. We leave a more detailed study of this class of observables as future work, including an operational definition in terms

to treat the full SU(3) structure for each subsequent emission.

A major conclusion is that standard LEP-observables, including event shapes and jet rates, are only affected by at most a few percent. For a class of observables dividing the event into a hard reference system and accompanying radiation we expect larger differences. This is indeed seen for tailored observables like the average transverse momentum with respect to a thrust axis determined by a system of three hardest partons, in case of which we see deviations as large as 20%.

The small differences can, in the case of the standard observables, largely be explained by the fact that these observables are either sensitive to collinear radiation, or to the first hard emissions.

Another contributing factor is that the color suppressed terms can be seen to be quite small from considerations of color space alone, when starting from a $q\bar{q}$ -pair. This is not the case if the hard scattering process is e.g. QCD $2 \rightarrow 2$. In this case we may see more striking differences between the approximations considered, though we cannot yet make a definite statement. The simulation framework is general enough to cope with this case and we leave a detailed discussion of subleading N_c effects at hadron colliders to future work.

In addition to what is presented here, there are several other effects which should be included before it can be claimed that a parton shower fully simulates SU(3) physics. Apart from including a running coupling constant and the $g \rightarrow q\bar{q}$ splitting kernel, we like to include virtual color rearranging gluon exchanges. We view this work as a proof of concept, and a first step towards quantifying the impact of subleading N_c contributions.

Finally, the parton shower outcome should be hadronized. While this is in itself an interesting task, it is much beyond the scope of the present paper. In an ordinary parton shower, where the shower outcome corresponds to a well defined probabilistic color line arrangement, this color structure is fed into the hadronization model. Here, the state after showering contains amplitude level information, and can thus not simply be input into existing hadronization models. While studying the influence of the hadronization on the parton shower outcome is an interesting task, we thus refrain from it at this stage.

Acknowledgments

We are grateful to Yuri Dokshitzer, Stefan Gieseke, Leif Lönnblad and Zoltan Nagy for discussions on this subject. We would also like to thank Markus Diehl, Stefan Gieseke, Gösta Gustafson and Torbjörn Sjöstrand for comments on the manuscript. S.P. acknowledges the kind hospitality of the Theoretical High Energy Physics group at Lund where this work was completed, and funding by the Helmholtz Alliance “Physics at the Terascale”. M.S. was supported by the Swedish Research Council (contract number 621-2010-3326).

References

- [1] T. Sjöstrand, S. Mrenna, and P. Skands, *A Brief Introduction to PYTHIA 8.1*, *Comput. Phys. Commun.* **178** (2008) 852–867, [[arXiv:0710.3820](#)].
- [2] M. Bähr et al., *Herwig++ Physics and Manual*, *Eur. Phys. J.* **C58** (2008) 639–707, [[arXiv:0803.0883](#)].
- [3] T. Gleisberg et al., *SHERPA 1.alpha, a proof-of-concept version*, *JHEP* **02** (2004) 056, [[hep-ph/0311263](#)].
- [4] L. Lönnblad, *Correcting the colour-dipole cascade model with fixed order matrix elements*, *JHEP* **05** (2002) 046, [[hep-ph/0112284](#)].
- [5] F. Krauss, *Matrix elements and parton showers in hadronic interactions*, *JHEP* **08** (2002) 015, [[hep-ph/0205283](#)].
- [6] S. Hoeche, F. Krauss, N. Lavesson, L. Lonnblad, M. Mangano, et al., *Matching parton showers and matrix elements*, [hep-ph/0602031](#).
- [7] N. Lavesson and L. Lönnblad, *Merging parton showers and matrix elements – back to basics*, *JHEP* **04** (2008) 085, [[arXiv:0712.2966](#)].
- [8] S. Hoeche, F. Krauss, S. Schumann, and F. Siegert, *QCD matrix elements and truncated showers*, *JHEP* **05** (2009) 053, [[arXiv:0903.1219](#)].
- [9] K. Hamilton, P. Richardson, and J. Tully, *A modified CKKW matrix element merging approach to angular-ordered parton showers*, [arXiv:0905.3072](#).
- [10] M. Dobbs, *Phase space veto method for next-to-leading order event generators in hadronic collisions*, *Phys. Rev.* **D65** (2002) 094011, [[hep-ph/0111234](#)].
- [11] S. Frixione and B. R. Webber, *Matching NLO QCD computations and parton shower simulations*, *JHEP* **06** (2002) 029, [[hep-ph/0204244](#)].
- [12] P. Nason, *A new method for combining NLO QCD with shower Monte Carlo algorithms*, *JHEP* **11** (2004) 040, [[hep-ph/0409146](#)].
- [13] Z. Nagy and D. E. Soper, *Matching parton showers to NLO computations*, *JHEP* **10** (2005) 024, [[hep-ph/0503053](#)].
- [14] S. Frixione, F. Stoeckli, P. Torrielli, and B. R. Webber, *NLO QCD corrections in Herwig++ with MC@NLO*, *JHEP* **1101** (2011) 053, [[arXiv:1010.0568](#)].
- [15] S. Platzer and S. Gieseke, *Dipole Showers and Automated NLO Matching in Herwig++*, [arXiv:1109.6256](#).
- [16] Z. Nagy and D. E. Soper, *A new parton shower algorithm: Shower evolution, matching at leading and next-to-leading order level*, [hep-ph/0601021](#).

- [17] J.-C. Winter and F. Krauss, *Initial-state showering based on colour dipoles connected to incoming parton lines*, *JHEP* **07** (2008) 040, [[arXiv:0712.3913](#)].
- [18] M. Dinsdale, M. Ternick and S. Weinzierl, *Parton showers from the dipole formalism*, *Phys. Rev.* **D76** (2007) 094003, [[arXiv:0709.1026](#)].
- [19] S. Schumann and F. Krauss, *A Parton shower algorithm based on Catani-Seymour dipole factorisation*, *JHEP* **03** (2008) 038, [[arXiv:0709.1027](#)].
- [20] S. Platzer and S. Gieseke, *Coherent Parton Showers with Local Recoils*, *JHEP* **01** (2011) 024, [[arXiv:0909.5593](#)].
- [21] G. Gustafson and U. Pettersson, *Dipole Formulation of QCD Cascades*, *Nucl.Phys.* **B306** (1988) 746.
- [22] Z. Nagy and D. E. Soper, *Parton showers with quantum interference*, *JHEP* **09** (2007) 114, [[arXiv:0706.0017](#)].
- [23] M. Sjö Dahl, *Color structure for soft gluon resummation: A General recipe*, *JHEP* **0909** (2009) 087, [[arXiv:0906.1121](#)].
- [24] M. Sjö Dahl, *Color evolution of $2 \rightarrow 3$ processes*, *JHEP* **0812** (2008) 083, [[arXiv:0807.0555](#)].
- [25] M. Sjö Dahl, *ColorFull – A C++ package for color space calculations, work in progress*.
- [26] S. Platzer and M. Sjö Dahl, *The Sudakov Veto Algorithm Reloaded*, [arXiv:1108.6180](#).
- [27] S. Catani and M. Seymour, *The Dipole formalism for the calculation of QCD jet cross-sections at next-to-leading order*, *Phys.Lett.* **B378** (1996) 287–301, [[hep-ph/9602277](#)].
- [28] S. Catani and M.H. Seymour, *A general algorithm for calculating jet cross sections in NLO QCD*, *Nucl. Phys.* **B485** (1997) 291–419, [[hep-ph/9605323](#)].
- [29] M. H. Seymour, *Matrix element corrections to parton shower algorithms*, *Comp. Phys. Commun.* **90** (1995) 95–101, [[hep-ph/9410414](#)].
- [30] E. Norrbin and T. Sjöstrand, *QCD radiation off heavy particles*, *Nucl. Phys.* **B603** (2001) 297–342, [[hep-ph/0010012](#)].
- [31] Y. I. Azimov, Y. L. Dokshitzer, V. A. Khoze, and S. Troian, *The String Effect and QCD Coherence*, *Phys.Lett.* **B165** (1985) 147–150.